IOPscience iopscience.iop.org

Home Search Collections Journals About Contact us My IOPscience

# A gradational system for ferroelectric nanosized $(Pb_{0.7}Sr_{0.3})TiO_3$ particles

This article has been downloaded from IOPscience. Please scroll down to see the full text article.

2009 J. Phys.: Condens. Matter 21 025903

(http://iopscience.iop.org/0953-8984/21/2/025903)

View the table of contents for this issue, or go to the journal homepage for more

Download details:
IP Address: 129.252.86.83
The article was downloaded on 29/05/2010 at 17:03

Please note that terms and conditions apply.

J. Phys.: Condens. Matter **21** (2009) 025903 (6pp) doi:10.1088/0953-8984/21/2/025903

# A gradational system for ferroelectric nanosized $(Pb_{0.7}Sr_{0.3})TiO_3$ particles

**Fumihito Shikanai[1,2], Jun Kano[2], Hiroshi Sawa[1], Fan Zhang[3], Tomoaki Karaki[4], Masatoshi Adachi[4], Je-Geun Park[1,5], Seiji Kojima[2], Susumu Ikeda[1] and Takashi Kamiyama[1]**

[1] Institute of Materials Structure Science, High Energy Accelerator Research Organization, Tsukuba, Ibaraki 305-0801, Japan
[2] Graduate School of Pure and Applied Sciences, University of Tsukuba, Tsukuba, Ibaraki 305-8573, Japan
[3] School of Materials Science and Engineering, Shenyang Institute of Chemical Technology, Shenyang 110142, People's Republic of China
[4] Department of Intelligent Systems Design Engineering, Toyama Prefectural University, Imizu, Toyama 939-0398, Japan
[5] Department of Physics, Sungkyunkwan University, Suwon 440-746, Korea

Received 1 September 2008, in final form 16 November 2008
Published 11 December 2008
Online at stacks.iop.org/JPhysCM/21/025903

**Abstract**
Synchrotron radiation x-ray diffraction measurement was performed to investigate the size effect in ferroelectric nanosized $(Pb_{0.7}Sr_{0.3})TiO_3$ particles with various sizes ranging from 10 to 200 nm. The 200 and 002 Bragg reflections were separated using low energy synchrotron radiation x-rays. The peak profiles of the 002 reflections show a large broadening and asymmetry for all particle sizes compared with those of the 200 reflections. These anomalously wide and asymmetric peak profiles become marked for peaks with a large $l$. The aspect ratio of the lattice constants $c/a$ and the atomic distance between the anions and cations decrease gradually in the vicinity of the surface of the particles, indicating that the asymmetrical profiles can be attributed to the formation of a gradational system.

(Some figures in this article are in colour only in the electronic version)

## 1. Introduction

Recently, technologies for controlling various nanosized materials, such as wires, thin films, colloidal particles, nanotubes, and fullerenes, have been progressing rapidly [1–4]. These materials are expected to exhibit a quantum effect owing to their sizes. On the other hand, perovskite ferroelectrics have attracted much attention because of their advantages of piezoelectricity and ferroelectricity, for use in devices. Technologies for forming minute particles such as ferroelectric materials with uniform high performance have also advanced. In the nanoscale region, ferroelectric materials show many unique and interesting phenomena that are collectively known as 'the size effect'. Their dielectric constants at room temperature (RT) depend significantly on the grain size. Arlt *et al* [5] performed dielectric measurements on fine-grained $BaTiO_3$ (BT) with grain sizes of 300 nm–100 $\mu$m. The maximum dielectric constant due to the domain size effect of the 90° domain was observed at grain sizes of 700 nm–1 $\mu$m; however, the dielectric constant decreased markedly with decreasing grain size for grains less than 700 nm in size. Michael *et al* [6] calculated the spontaneous polarization hysteresis loop of a ferroelectric nanocluster and showed that its coercive field, remanent polarization and phase transition temperature depend on the particle size, and that particle characteristics are sensitive to the interaction strength at the surface and the strength of the microscopic coupling to defects. They also reported the influence of doping effects on the properties of ferroelectric nanoparticles [7]. Morozovska *et al* [8] performed a phenomenological theoretical calculation taking into account the depolarization field and effect of surface stress, and showed that the size effect depends on the particle shape. In addition to these studies, it has been reported that the ferroelectricity of BT nanowires disappears below a critical diameter of about 1.2 nm [9]. It has also been found that a misfit in the lattice constant between the base material

 © 2009 IOP Publishing Ltd Printed in the UK

and the ferroelectric thin film enhances the ferroelectricity and induces a new phase [10, 11].

On the other hand, from the viewpoint of crystal structure, nanosized particles have an inhomogeneous internal microscopic structure. Arlt *et al* [5] also performed x-ray measurements on fine-grained BT, and found 'pseudo-cubic' reflections from a sample with a grain size of 800 nm. Recently, Aoyagi *et al* [12] performed synchrotron radiation (SR) x-ray diffraction measurements on BT nanoparticles. The diffraction peak profiles were well explained by the core–shell model in which a tetragonal core is covered by a thin cubic shell originating from the surface effect. The volume ratio of the cubic phase to the tetragonal phase depends on the particle size, while the thickness of the cubic shell is independent of it and is estimated to be 8 nm. This result indicates that the phase transition of BT disappears at a particle size of less than 16 nm. Thus, x-ray diffraction offers an advantage as regards statistical accuracy in observing the internal structure and lattice; however, clear observation of dipoles is difficult because they appear as small displacements of Ti and O atoms. It is particularly impossible to observe local dipoles. In contrast, interesting phenomena in the vicinity of the surface (or domain boundary) collectively known as 'depolarizing' have been reported via theoretical approaches [13–16]. Chaib *et al* [15] performed a theoretical calculation based on the orbital approximation in correlation with the dipole–dipole interaction for the BT system. They reported that spontaneous polarization is markedly suppressed near the *c* surfaces. Other reports showed similar results regarding the behavior of spontaneous polarization in the vicinity of the surface [13, 14, 16]. However, these reports did not mention the lattice, because the calculations were performed for a constant volume system using the bulk lattice constants. It is naturally expected that the lattice constants decrease in the vicinity of the surface, and that this is accompanied by depolarization. Recently, such a gradational lattice system has been observed in the vicinity of a 180° nanodomain boundary of the Rochelle salt in alumina pores [17] and at the domain boundary of a triple layer for $SrTiO_3/PbZr_{0.2}Ti_{0.8}O_3/SrTiO_3$ [18]. Thus, transmission electron microscopy (TEM) is suitable for clear observation of the local lattice and structure in the vicinity of the surface; however, it is not ideal for the study of internal structure. As an alternative method, details of gradation in the vicinity of the surface on $PbTiO_3$ thin films have been reported by employing x-ray photoelectron diffraction [19].

The situations suggest that the structure of nanoparticles remains unclear without complementary theoretical calculations and experimental measurements of the local and internal structures. Such gradational systems, which have been observed on the surface of thin films and at domain boundaries, are also expected to be observed in nanoparticles. Therefore, in order to clarify these size effects and structural details of ferroelectric nanoparticles, we select the $(Pb_xSr_{1-x})TiO_3$ (PST) solid-solution nanosystem, which is expected to exhibit a large deformation at RT, as a sample for SR x-ray observation. Furthermore, to obtain high resolution, a low energy, low wavelength incident beam was used in the SR x-ray measurement. In this paper, we show the diffraction pattern of the $(Pb_{0.7}Sr_{0.3})TiO_3$ (PST7/3) nanosystem using high resolution SR x-ray measurement and discuss the structural details on the basis of various broadenings and Rietveld analysis.

The PST system exhibits potentially useful ferroelectric properties. The phase transition temperature ($T_C$) can be controlled continuously over an extremely wide temperature range from 0 to 763 K by adjusting the Sr ratio [20–22]. This characteristic is attractive for application in tunable microwave devices and dynamic random access memory (DRAM) devices [23, 24]. The solid-solution system changes from tetragonal to cubic at RT when the Sr ratio is less than 0.5 [25]. PST7/3 powder was produced by a simple coprecipitation method, and various particle sizes from 10 to 200 nm were prepared by adjusting the calcination temperature [26, 27]. The samples showed a marked size effect; $T_C$ decreased by more than 150 K with decreasing particle size. Furthermore, confined phonon modes were observed in a nanosized PST7/3 system by Raman scattering [28]. Structural characterization is vital for developing dynamical properties, which are unique to nanosized materials.

## 2. Experiment

The measurement was performed on a multipurpose Weissenberg-type imaging plate diffractometer installed at BL-1B in the photon factory of the High Energy Accelerator Research Organization. To separate the 200 and 002 reflections and measure full Bragg peak profiles, the incident beam energy selected was the lowest possible energy of 8 keV with a wavelength $\lambda = 1.547$ Å. Five samples of PST7/3 with particle sizes of 10, 25, 50, 100 and 200 nm were enclosed in glass capillaries with a bore size $2r = 0.3$ mm. Prior to the SR x-ray measurement, the average particle sizes of these samples were estimated using a transmission electron microscope [26, 27]. Silicon powder was also prepared as a standard sample. Diffraction data were recorded at RT. Rietveld analyses were performed up to $2\theta = 140°$ for the collected data. The $d$ range from $d = 0.82$ to 4.46 Å was sufficient for the Rietveld analysis. The resolutions in the region of low $2\theta$ and high $2\theta$ angles were estimated from the full width at half-maximum (FWHM) of a standard sample as 0.07° and 0.13°, respectively.

## 3. Results and discussion

### *3.1. Mean structure*

Figure 1(a) shows the particle size dependences of the 200 and 002 reflections. Size-induced broadening accompanied by a decrease in the particle size can be observed clearly for both reflections. The 002 reflections can be observed even in the data for the 10 nm sample, as shown in figure 1(a); therefore, the PST7/3 system for all the samples measured belongs to a ferroelectric tetragonal system. The peak position of the 200 reflections shifts gradually to a lower $2\theta$ angle with decreasing particle size. Figure 1(b) shows the particle size dependence of the lattice constants $a$ and $c$ obtained from the Rietveld

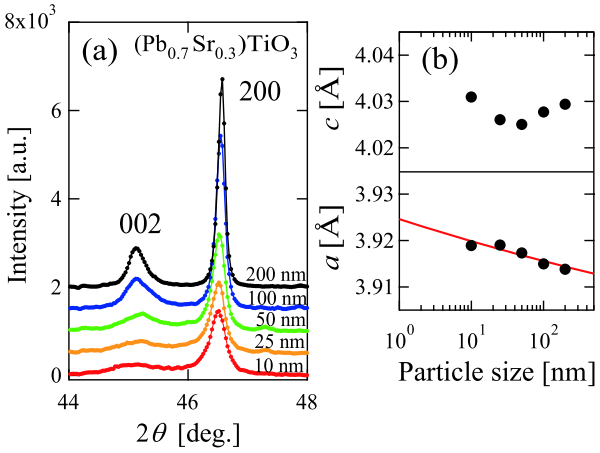


**Figure 1.** (a) Particle size dependences of the 200 and 002 Bragg reflections. (b) Lattice constants obtained from Rietveld analysis.

refinement using a conventional model of a single tetragonal phase with the space group $P4mm$. The lattice constant $a$ shows an exponential increase with decreasing particle size, as shown in figure 1(b). This shows that the increase in $a$ mainly causes size-induced volume expansion [29] as a function of $a^2$. In striking contrast, the lattice constant $c$ seems to be independent of the particle size. Similar particle size dependences of both lattice constants for particle sizes below 100 nm have been reported for a BT nanoparticle system [30]. This unique particle size dependence of $c$ is considered to be caused by the balance between a decrease in $c$ with the suppression of spontaneous polarization at RT and an increase in $c$ due to size-induced volume expansion. This suggests that the nature of nanoparticles is relevant to their polarization. The FWHM of the 002 reflections is wider than that of the 200 reflections, as shown in figure 1(a). This indicates that $c$ is diffusive and inhomogeneous in the nanoparticle samples compared with $a$. In addition, the peak profiles of the 002 reflections are asymmetric whereas the 200 reflections are nearly symmetric.

### *3.2. Size- and strain-induced broadening*

A method of separating size- and strain-induced broadening has been developed by Williamson and Hall [31] and is now known as the Williamson–Hall plot method. Figure 2(a) shows a Williamson–Hall plot for PST7/3 with a particle size of 200 nm. $\beta$ is the FMWH of the reflection, which is obtained by subtracting instrumental broadening from the observed FWHM using $\beta = (\beta_{\rm obs}^2 - \beta_{\rm inst}^2)^{1/2}$, where $\beta_{\rm inst}$ is estimated from the Gaussian component of the profile, $\beta_{\rm inst} = [8\ln 2(U\tan^2\theta + V\tan\theta + W)]^{1/2}$, using the parameters obtained from the Rietveld analysis: $U = 0.002\,0999$, $V = -0.000\,5099$ and $W = 0.001\,9868$. The slope in the figure gives the weighted average strain $\varepsilon_{\rm str}$ while the $y$ intercept gives $0.9\lambda/L$, where $L$ is the crystallite size. As shown in figure 2(a), both the slope and the $y$ intercept depend on $l$. The $l$ dependences of $\varepsilon_{\rm str}$ and $L$ are shown in the inset of figure 2(a). $\varepsilon_{\rm str}$ increases with increasing $l$; this corresponds to the anisotropic broadening of Bragg reflections

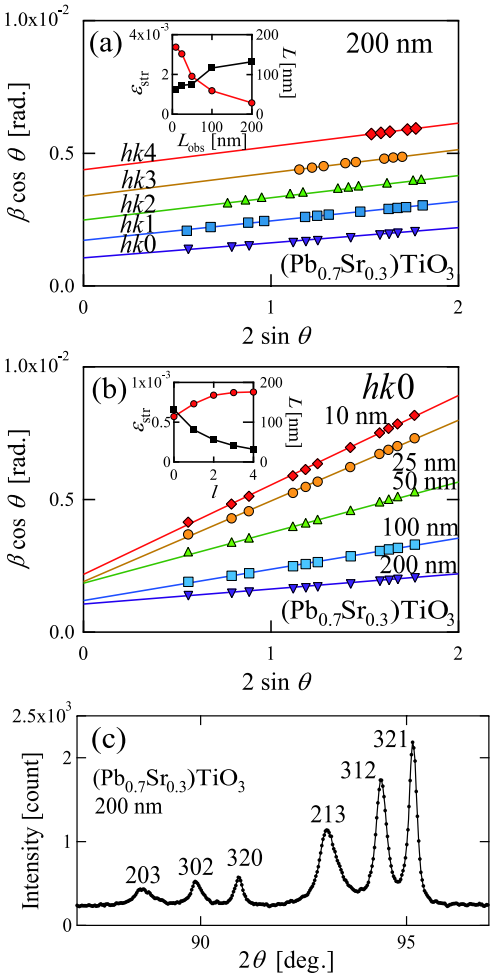


**Figure 2.** (a) Williamson–Hall plot for PST7/3 nanoparticles 200 nm in size. The slope corresponds to the weighted average strain $\varepsilon_{\rm str}$, and the $y$ intercept gives $0.9\lambda/L$ ($L$: crystallite size).
(b) Williamson–Hall plot using $hk0$ reflections for various particle sizes of PST7/3. (c) Diffraction pattern in the region of high $2\theta$ angle.

towards the $c^*$ axis direction. The $L$ estimated from the $y$ intercept shows a decrease against $l$; however, the result is inconsistent with the particle shape observed by TEM, which is a rectangular parallelepiped growing in the $c$ axis direction. Therefore, to estimate the particle size excluding the effect of anisotropic broadening, the reflections with an index of $hk0$ were used. Figure 2(b) exhibits a Williamson–Hall plot using $hk0$ reflections for various particle sizes of PST7/3. As shown in the figure, the $hk0$ reflections of each particle size show a linear tendency, and the slope depends on the size. $\varepsilon_{\rm str}$ shows an exponential increase from 0.057(2)% to 0.338(3)% with decreasing particle size, as shown in the inset of figure 2(b), where the numbers in parentheses are standard deviations. The $y$ intercept shows an increase with decreasing particle size. The estimated $L$ values are 132.0(3) nm, 116.6(3) nm, 75.4(2) nm, 73.2(2) nm and 64.1(2) nm for samples with particle sizes of 200 nm, 100 nm, 50 nm, 25 nm and 10 nm, respectively. The particle size dependence of $L$ is plotted in the inset of figure 2(b). As mentioned above, broadening of the 200 reflections shown in figure 1(a) originates from

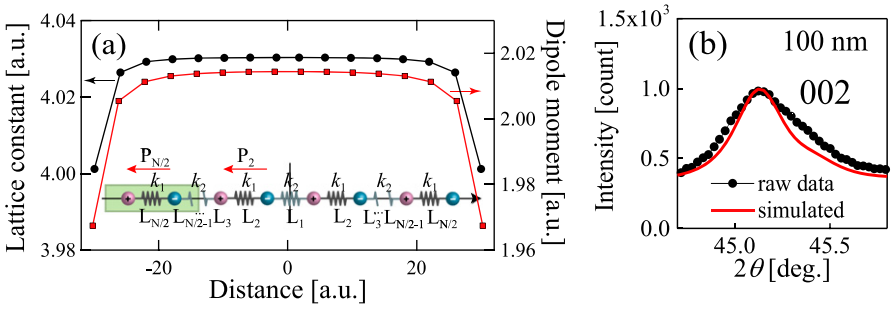


**Figure 3.** (a) Lattice constant and dipole moment calculated from the 1D dipole system illustrated in the figure. (b) Simulated profile of 002 reflection using lattice constant $c$ obtained from calculation.

size- and strain-induced broadenings. However, comparing figure 2(a) with 2(b), in spite of $\varepsilon_{\rm str}$ being about 1/4, the PST7/3 nanoparticle system still has a large FWHM as an anisotropic broadening towards the $c^*$ axis, which is not comparable to the FWHM of the 10 nm sample. In addition, very asymmetric peak profiles were obtained for peaks with a large $l$, as shown in figure 2(c). These results show that another crystallographic broadening mechanism exists for the nanoparticle. Thus, we focused on the asymmetric profiles of 002, which have a close relationship with the distributions of $c$ in the direction of dipole moments inside the particles.

### *3.3. Asymmetric broadening*

We now discuss some possible origins of the asymmetrical 002 reflection. First, we assumed a Gaussian distribution of the particle sizes of the samples, which have various particle sizes at different lattice constants. However, this assumption cannot account for the asymmetry of the 002 reflections, because the particle size dependences of both $a$ and $c$ are extremely weak (about 0.25%), as shown in figure 1(b). Next, we performed Rietveld analysis using the core–shell model. The volume ratio of the tetragonal system to the cubic system obtained was 0.987:0.013 from the data for a particle size of 200 nm, although some cubic peaks were inconsistent with the observed data in the high $2\theta$ region. Finally, we examined the depolarizing dipole and gradational lattice mentioned above. In the case of a gradational lattice and a structure system existing along the $c$ direction, the diffraction peak of 002 is represented as follows. When the lattice vector of the $m$th unit cell is $\mathbf{c}_m = \mathbf{c} - \Delta\mathbf{c}_m$, the reciprocal lattice vector $\mathbf{c}_m^*$ becomes

$$\mathbf{c}_m^* = \frac{\mathbf{a}\times\mathbf{b}}{V - \Delta V_m},$$

where $\Delta V_m = \Delta\mathbf{c}_m \cdot (\mathbf{a}\times\mathbf{b})$. Then, $\mathbf{c}_m^*$ takes the form

$$\mathbf{c}_m^* = \mathbf{c}^* \sum_{n=0} \left(\frac{\Delta V_m}{V}\right)^n. \tag{1}$$

The inner product of the wavevector $\mathbf{k}_m$ and the position vector $\mathbf{r}_m$ depends only on $z_m$:

$$\begin{aligned}\mathbf{k}_m \cdot \mathbf{r}_m &= (h\mathbf{a}^* + k\mathbf{b}^* + l\mathbf{c}_m^*)\cdot(x\mathbf{a} + y\mathbf{b} + z_m\mathbf{c}_m)\\ &= \mathbf{k}\cdot\mathbf{r} + l(z_m - z).\end{aligned} \tag{2}$$

The intensity is proportional to $F^2$; hence,

$$\begin{aligned}I &\propto \left(\sum_{m'} F_{m'}^*\right)\left(\sum_m F_m\right)\\ &= \sum_{m=m'} F_m^2 + 2\sum_{m<m'} \exp[2\pi i l(z_m - z_{m'})],\end{aligned} \tag{3}$$

where the atomic structure factors are omitted from $F_m$ to give a simple subscript of the $m$th unit cell, as in $F_m = \exp\{2\pi i \mathbf{k}_m \cdot \mathbf{r}_m\}$. In this system, the dipole decreases gradually toward the surface, an thereby we approximate that $z_{m'} - z_m \simeq p\Delta z$ ($p$: integer); the second term of equation (3) becomes the Laue function and is identical to $(2N+1)\delta(\Delta z) - 1$, where $N$ is the total number of unit cells. However, the spectrum cannot be observed, because the diffraction angle from the $m$th unit cell shifts to satisfy

$$c_m \sin\theta_m = c\sin\theta. \tag{4}$$

Hence, the diffraction profile can be obtained using a simple sum of reflection intensities from each unit cell. The difference in $c$ appears as the difference of scattering angle $2\theta$, and the intensity at $2\theta_m$ is in proportion to the square of the number of unit cells, which have the same lattice constant and structure. To estimate the diffraction peak profile of the 002 reflection, we used a fundamental system constructed from inline dipole series and springs, as illustrated in figure 3(a). A similar 2D system has been proposed by Baudry and Tournier [13]. The 1D system is sufficient to show the asymmetry of the 002 reflection, because the 002 reflection includes no information on the $a$ and $b$ axis directions. The length for an even number of springs, $L_{\rm N/2}$, is proportional to the size of the local dipole moment. That for an odd number of springs works as the strain without changing the local dipole moment. The local lattice constant is obtained from $L_{\rm N/2-1} + L_{\rm N/2}$. The force constants $k_1$ and $k_2(=k)$ are equal for simplification. The result depends on the initial length of the springs $L_{\rm initial}$ and the ratio of the force constant $k$ to the coefficient of the Coulomb force $(4\pi\varepsilon_0)^{-1}(Ze)^2$, where the ratio is simplified to 1. The result shown in figure 3(a) was obtained using 32 charges and $L_{\rm initial} = 2.1$. The dipole moment and lattice constant gradually decrease from the center to the end of the chain, as shown in figure 3(a). The result shows the same tendency as the results of depolarization [13–16]. Figure 3(b) shows the simulated peak profile for the 002 reflection using the results for $c$. The profile curve of 002 was obtained from the simple

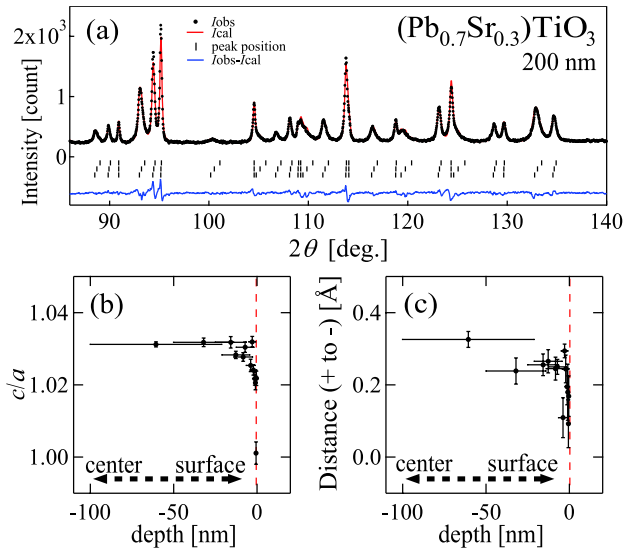


**Figure 4.** (a) Representative result of a fitting pattern. (b) Aspect ratio $c/a$, as a function of depth estimated from the volume ratio and product size. (c) Distance from positive charge to negative charge as a function of depth.

**Table 1.** Results of Rietveld analysis. All the atomic positions are expressed as in $z$ coordinates. Other atomic positions are equal to 0. Standard deviations are in parentheses.

| (nm) | 200 | 100 | 50 | 25 | 10 |
|---|---|---|---|---|---|
| $R_{wp}$ | 6.72 | 5.98 | 6.77 | 8.68 | 7.08 |
| $S$ | 1.37 | 1.26 | 1.32 | 1.37 | 1.32 |
| $a$ (Å) | 3.9138(4) | 3.91496(7) | 3.9173(1) | 3.9190(1) | 3.9189(1) |
| $c_1$ (Å) | 4.0358(2) | 4.0395(3) | 4.0418(3) | 4.0382(3) | 4.0438(3) |
| $Ti^{4+}1$ | 0.528(4) | 0.547(3) | 0.549(2) | 0.539(3) | 0.535(3) |
| $O^{2-}11$ | 0.600(3) | 0.587(6) | 0.591(1) | 0.577(5) | 0.589(4) |
| $O^{2-}12$ | 0.100(5) | 0.096(8) | 0.106(8) | 0.110(5) | 0.110(5) |
| $V$ (%) | 49.18 | 37.59 | 40.81 | 61.77 | 61.66 |
| $c_2$ (Å) | 4.0245(2) | 4.0236(2) | 4.0168(3) | 3.9999(4) | 4.0044(4) |
| $Ti^{4+}2$ | 0.521(2) | 0.522(3) | 0.528(2) | 0.531(4) | 0.529(4) |
| $O^{2-}21$ | 0.578(3) | 0.568(3) | 0.536(2) | 0.570(8) | 0.576(7) |
| $O^{2-}22$ | 0.084(7) | 0.090(8) | 0.066(10) | 0.06(1) | 0.07(30) |
| $V$ (%) | 38.52 | 47.50 | 45.55 | | |
| $c_3$ (Å) | 4.0081(3) | 3.9998(4) | 3.9876(7) | | |
| $Ti^{4+}3$ | $=Ti^{4+}2$ | $=Ti^{4+}2$ | $=Ti^{4+}2$ | | |
| $O^{2-}31$ | $=O^{2-}21$ | $=O^{2-}21$ | $=O^{2-}21$ | | |
| $O^{2-}32$ | 0.07(2) | 0.054(8) | 0.054(5) | | |
| $V$ (%) | 12.30 | 14.91 | 13.64 | | |

sum of eight same-intensity reflections with different $2\theta$ using the profile of the 200 reflection. The profile is asymmetric and in good agreement with raw data. The results demonstrate that the gradational structure originates from self-balancing induced by the dipole interaction, and causes asymmetric profiles of the 002 reflection.

### *3.4. Rietveld refinement*

Rietveld refinement was performed using the multilayer model. Hoshina *et al* [32, 33] have proposed a similar gradational lattice multilayer model for the profiles of 002 and 200 reflections of BT nanoparticles. The model that we used divides nanoparticles with sizes of 200, 100 and 50 nm into three layers, and nanoparticles with sizes of 25 and 10 nm into two layers. This analytical model enables us to estimate the particle size from the FWHM of the Lorentzian components, because a couple of $c$ values covers the asymmetrical and anisotropic broadening in the $c^*$ direction. The lattice parameter $a$ was refined with restriction at the same value, while a couple of $c$ values was refined without restrictions. The profile function used in the analyses was the pseudo-Voigt function proposed by Thompson *et al* [34]. The space groups of all the layers have the same $P4mm$ tetragonal system. The calculated patterns are in good agreement with the observed data, with a goodness-of-fit indicator $S$ of about 1.3. Figure 4(a) shows a representative fitting in the high $2\theta$ region. The figure shows that the model can clearly reproduce the diffraction patterns, which depend on the index $l$ and have different sharpnesses and asymmetrical shapes. The results and the refined parameters with their standard deviations are listed in table 1. Particle size was estimated from a parameter of the Lorentzian component $X$, which is proportional to $(\cos\theta)^{-1}$, using the Scherrer formula $(180 \times 0.9\lambda)(\pi X)^{-1}$. The estimated particle sizes are 188(4), 124(3), 72(2), 61(2) and 54(2) nm for the samples with particle size of 200 nm, 100 nm, 50 nm, 25 nm and 10 nm, respectively. The results are consistent with those obtained from TEM [26, 27] and the Williamson–Hall method mentioned above. $c$ shows a gradual decrease with decreasing volume ratio for each particle size, as shown in table 1. The atomic positions of $Ti^{4+}$ and $O^{2-}$ also indicate gradational structures for each part. The aspect ratio of unit cells $c/a$ versus the depth from the surface is plotted in figure 4(b); here, the depth was estimated from the volume ratio and particle size. As shown in figure 4(b), the aspect ratio decreases slightly from the center of the particle and decreases rapidly at about 20 nm from the surface. Figure 4(c) shows the distances from the centers of the positive charges ($Pb^{2+}$, $Sr^{2+}$ and $Ti^{4+}$) to those of the negative charges ($O^{2-}$) obtained from the atomic positions. The distances show the same tendencies as the lattice, but the gradual change appears to extend up to the inner area of the particle. These results show that the PST7/3 nanoparticle has gradational lattices and a dipole system in the vicinity of the surface. Although the crystallographic cubic system is an inappropriate model for this PST7/3 system, it is proposed that such gradational lattices and dipoles correspond to the cubic shell and pseudo-cubic part.

## 4. Summary

In the present study, we showed various broadenings of reflections of the nanosized PST7/3 system (size-induced, strain-induced and anisotropic broadenings) through low energy SR x-ray diffraction, which can be used to separate each reflection in the powder diffraction pattern. Size-induced and strain-induced effects explained the broadening of the $hk0$ reflections, whereas wide and asymmetric broadening existed as anisotropic broadening in the $c^*$ direction. The gradational lattice and dipole in the vicinity of the surface reproduced the anomalously wide and asymmetric peak profiles depending on $l$. A gradual decrease in the lattice and dipoles in

the vicinity of the surface was also obtained by Rietveld analyses. Thus, we conclude that ferroelectric nanosized particles have gradational lattices and a dipole system in the vicinity of the surface, and such gradational lattices originate from self-balancing due to dipole interactions. The gradational system is considered to be a universal feature of nanosized ferroelectric materials. However, the future of the system is still unclear as regards particle, temperature and composition dependence. It is expected that the system could be controlled easily by adjusting the particle size and composition. In addition, the results indicate that the particle shape is closely related to the dipole, because the depolarized dipole depends on the number of unit cells along the *c* axis. This generates renewed interest in the dynamics of gradational systems [35]. The control of such gradational systems provides a potential method for discovering new phenomena in nanosized ferroelectric materials. Future investigations will be performed for characterizing and understanding the nature of nanosized ferroelectric materials.

## Acknowledgments

The authors express their gratitude to Dr N L Yamada for helpful discussions that gave us important inspiration and for significant contributions to this work. This work was supported in part by the Murata Science Foundation.

## References

[1] Sun H P, Tian W, Pan X Q, Haeni J H and Schlom D G 2004 *Appl. Phys. Lett.* **84** 3298
[2] Hart S J and Terray A V 2003 *Appl. Phys. Lett.* **83** 5316
[3] Luo Y, Szafraniak I, Zakharov N D, Nagarajan V, Steinhart M, Wehrspohn R B, Wendorff J H, Ramesh R and Alexe M 2003 *Appl. Phys. Lett.* **83** 440
[4] Sawa H, Wakabayashi Y, Murata Y, Murata M and Komatsu K 2005 *Angew. Chem. Int. Edn* **44** 1981
[5] Arlt G, Hennings D and de With G 1985 *J. Appl. Phys.* **58** 1619
[6] Michael Th, Trimper S and Wesslinowa J M 2006 *Phys. Rev.* B **74** 214113
[7] Michael Th, Trimper S and Wesslinowa J M 2008 *Ferroelectrics* **363** 110
[8] Morozovska A N, Glinchuk M D and Eliseev E A 2007 *Phys. Rev.* B **76** 014102
[9] Geneste G, Bousquet E, Junquera J and Ghosez P 2006 *Appl. Phys. Lett.* **88** 112906
[10] Choi K J, Biegalski M, Li Y L, Sharan A, Schubert J, Uecker R, Reiche P, Chen Y B, Pan X Q, Gopalan V, Chen L Q, Schlom D G and Eom C B 2004 *Science* **306** 1005
[11] Pertsev N A, Tagantsev A K and Setter N 2000 *Phys. Rev.* B **61** R825
[12] Aoyagi S, Kuroiwa Y, Sawada A, Yamashita I and Atake T 2002 *J. Phys. Soc. Japan* **71** 1218
[13] Baundy L and Tournier J 2001 *J. Appl. Phys.* **90** 1442
[14] Kretschmer R and Binder K 1979 *Phys. Rev.* B **20** 1065
[15] Chaib H, Eng L M, Schlaphof F and Otto T 2005 *Phys. Rev.* B **71** 085418
[16] Zhou Y and Shin F G 2006 *J. Appl. Phys.* **100** 024101
[17] Yadlovker D and Berger S 2005 *Phys. Rev.* B **71** 184112
[18] Jia C L, Mi S B, Urban K, Vrejoiu I, Alexe M and Hesse D 2008 *Nat. Mater.* **7** 57
[19] Despont L, Koitzsch C, Clerc F, Garnier M G, Aebi P, Lichtensteiger C, Triscone J M, Garcia de Abajo F J, Bousquet E and Ghosez Ph 2006 *Phys. Rev.* B **73** 094110
[20] Meng J, Zou G, Ma Y, Wang X and Zhao M 1994 *J. Phys.: Condens. Matter* **6** 6549
[21] Lemanov V V, Smirnova E P and Tarakanov E A 1997 *Phys. Solid State* **39** 628
[22] Somiya Y, Bhalla A S and Cross L E 2001 *Int. J. Inorg. Mater.* **3** 709
[23] Chung H J, Chung S J, Kim J H and Woo S I 2001 *Thin Solid Films* **394** 213
[24] Jain M, Majumder S B, Guo R, Bhalla A S and Katiyar R S 2002 *Mater. Lett.* **56** 692
[25] Kuo S Y, Li C T and Hsieh W F 2002 *Appl. Phys. Lett.* **81** 3019
[26] Zhang F, Karaki T and Adachi M 2005 *Japan. J. Appl. Phys.* **44** 6995
[27] Zhang F, Karaki T, Adachi M and Li S 2006 *Japan. J. Appl. Phys.* **45** 1873
[28] Kano J, Tsukada S, Zhang F, Karaki T, Adachi M and Kojima S 2007 *Japan. J. Appl. Phys.* **46** 7148
[29] Matsubara T and Kamiya K 1977 *Japan. J. Appl. Phys.* **58** 767
[30] Hoshina T, Kakemoto H, Tsurumi T, Wada S and Yashima M 2006 *J. Appl. Phys.* **99** 054311
[31] Williamson G K and Hall W H 1953 *Acta Metall.* **1** 22
[32] Hoshina T, Wada S, Kuroiwa Y, Kakemoto H and Tsurumi T 2007 *Proc. of 16th IEEE Int. Symp. Applications, Ferroelectrics* p 476
[33] Hoshina T, Wada S, Kuroiwa Y and Tsurumi T 2008 *Appl. Phys. Lett.* **93** 192914
[34] Thompson P, Cox D E and Hastings J B 1987 *J. Appl. Crystallogr.* **20** 79
[35] Xiao J J, Yakubo K and Tu K W 2006 *Appl. Phys. Lett.* **88** 241111